S

Caliphate Journal of Science & Technology (CaJoST)

ISSN: 2705-313X (PRINT); 2705-3121 (ONLINE) Research Article

Open Access Journal available at: https://cajost.com.ng/index.php/files and https://www.ajol.info/index.php/cajost/index

DOI: https://dx.doi.org/10.4314/cajost.v8i1.9

Article Info

Received: 21st January 2026

Revised: 26th February 2026

Accepted: 16th March 2026

The Potential of Sawdust-Derived Graphene-Like Carbon for Crude Oil Spill Remediation

Mansur Y. Ibrahim*, Hassana A. Musa and Hadi Sulaiman

Department of Pure and Industrial Chemistry, Sokoto State University, Sokoto, Nigeria

***Corresponding author's email:**

ymansur64@gmail.com

Oil spill contamination remains a significant environmental and socio-economic issue, driving the need for cost-effective and sustainable remediation materials. This study explores the synthesis of a graphene-like carbon material from sawdust, an abundant lignocellulosic waste, for crude oil spill remediation. The sawdust-derived graphene-like carbon (SD-GLC) was produced through controlled carbonization and chemical treatment to induce graphitic domain formation. Characterization using UV–Visible spectroscopy, Fourier transform infrared spectroscopy (FTIR), X-ray diffraction (XRD), and scanning electron microscopy (SEM) confirmed the transformation into a partially graphitized material with dominant sp^2 carbon structures and residual oxygen functional groups. Batch adsorption experiments assessed the influence of adsorbent dosage, contact time, and pH on oil removal efficiency. The SD-GLC demonstrated high crude oil removal performance, exceeding 95% under optimal conditions, particularly at contact times of 60–100 minutes and acidic pH levels (2.5–4.0). Adsorption followed pseudo-second-order kinetics and aligned more closely with the Freundlich isotherm model, indicating heterogeneous multilayer adsorption governed by surface interactions and pore filling. However, reusability tests showed a sharp decline in performance, with efficiencies dropping below 10% after regeneration due to irreversible oil entrapment, pore blockage, and structural degradation. Despite this limitation, SD-GLC shows strong potential as a low-cost, sustainable sorbent, with further modifications needed to improve recyclability and practical application.

Keywords: Crude oil; Sawdust; Graphene-like carbon; Adsorption; Oil spill remediation; Sustainability.

Cite this: *CaJoST*, 2026, 1, 75-86

1. Introduction

Oil spill contamination poses severe ecological and socio-economic risks, particularly in aquatic and coastal environments where petroleum hydrocarbons persist for extended periods and disrupt biological systems (ITOPF, 2023 and Liu et al., 2021) Conventional remediation methods such as mechanical skimming, in situ burning, and chemical dispersants are often costly, inefficient at low oil concentrations, and associated with secondary environmental impacts (Zhao et al., 2020). Adsorption-based remediation has emerged as a preferred alternative due to its operational simplicity, high efficiency, and potential for material recovery (Wang et al., 2023).

Carbon-based materials, including activated carbon, carbon nanotubes, and graphene-derived structures, have received considerable attention for oil spill remediation because of their high surface area, hydrophobicity, and tunable surface chemistry (Zhu et al., 2021). Among these, graphene-based sorbents show exceptional oil uptake capacities; however, their large-scale application is constrained by high production costs and environmentally intensive synthesis routes.

Biomass-derived graphitic materials offer a sustainable and economically viable alternative (Wang et al., 2023). Agricultural and forestry wastes such as sawdust, rice husk, coconut shell, and sugarcane bagasse are abundant carbon sources that can be converted into porous graphitic or graphene-like carbons through controlled thermal and chemical treatments (Zhang et al., 2024). Despite growing interest, many studies overstate graphene formation without sufficient structural evidence, and adsorption performance is frequently reported only as percentage removal, which limits comparison across studies.

This study addresses these gaps by synthesizing a graphene-like carbon material from sawdust and critically evaluating its crude oil adsorption performance using standardized metrics, controlled experimental conditions, and transparent statistical analysis.

2. Materials and Methods

2.1 Raw Material Preparation

Sawdust was collected from local wood-processing workshops in Sokoto, Nigeria, washed thoroughly with distilled water to remove dust, oils, and soluble impurities, and dried at 105 °C for 24 h. Biomass pre-cleaning (Figure 1) is known to significantly influence the uniformity and porosity of derived carbon materials (Kumar et al., 2021).

Figure 1: Saw dust samples preparation- Free saw dust and powdered Sawdust respectively

2.2 Carbonization and Chemical Treatment

The dried sawdust was carbonized in a muffle furnace at 600 °C for 2 h under limited oxygen conditions to produce biochar. Chemical treatment was then carried out using concentrated H_2SO_4 (98%) and $KMnO_4$ following a modified oxidation–reduction protocol similar to those reported for biomass-derived graphene-like carbons (Li et al., 2022). All reagent concentrations, reaction times, and washing steps were explicitly controlled and documented to ensure reproducibility and to minimize residual oxidants.

2.3 Characterization

UV–Vis spectroscopy, FTIR, XRD, and SEM were employed to assess optical, functional, and morphological properties. The material is consistently referred to as *graphene-like carbon*, acknowledging that Raman spectroscopy, X-ray photoelectron spectroscopy (XPS), and Brunauer–Emmett–Teller (BET) surface area analysis is required for definitive graphene confirmation and are recommended for future studies (Zhang et al., 2024).

2.4 Adsorption Experiments

2.4.1 Oil Concentration Determination

A simulated oil spill was prepared by dissolving 10.5 g of crude oil in 500 mL of water, corresponding to an initial concentration of 21,000 mg/L. Oil concentration was quantified using UV–Vis spectroscopy with a properly calibrated standard curve ($R^2 > 0.99$), incorporating appropriate dilution steps to remain within the linear detection range (Wang et al., 2023).

2.4.2 Experimental Design

Adsorption experiments followed a one-factor-at-a-time approach to isolate individual effects:

i. Dosage studies: adsorbent mass varied while contact time and pH were fixed.
ii. Contact time studies: time varied while dosage and pH were constant.
iii. pH studies: pH varied while dosage and contact time were constant.

This approach allows clearer interpretation of parameter effects, although multivariate optimization is recommended for future work.

2.4.3 Adsorption Capacity

Adsorption performance was calculated using equation (1):

$$q = \frac{(C_0 - C_e)V}{m} \quad (1)$$

where q is adsorption capacity (mg/g), C_0 and C_e are initial and equilibrium oil concentrations, V is solution volume, and m is adsorbent mass.

2.4.4 Reusability of Sawdust-Derived Graphene-Like Carbon Adsorbent

The reusability of the sawdust-derived graphene-like carbon (SD-GLC) adsorbent was evaluated to assess its operational stability and economic viability for repeated crude oil spill remediation applications. Reusability is a critical parameter for sorbent materials intended for large-scale environmental cleanup, as it directly influences material cost, waste generation, and long-term performance.

2.4.5 Adsorption–Desorption Cycles

Reusability tests were conducted through consecutive adsorption–desorption cycles using crude oil as the target contaminant. In each cycle, a fixed mass of SD-GLC (typically 0.1–0.5 g) was introduced into a known volume of crude oil–water mixture under ambient laboratory conditions. The system was gently agitated to ensure uniform contact between the adsorbent and oil phase, and the adsorption process was allowed to proceed until equilibrium was reached, as determined from preliminary kinetic studies.

After adsorption, the oil-laden adsorbent was separated from the aqueous phase by simple filtration. The amount of crude oil adsorbed was calculated gravimetrically using Equation (2):

$$q = \frac{m_f - m_i}{m_i} \quad (2)$$

Where q s the absorption capacity (g g^{-1}) m_i is the initial mass of the dry adsorbent and m_y is the mass after oil adsorption. This approach has been widely applied in evaluating oil sorbents due to its simplicity and reliability (Liu et al., 2017).

2.4.6 Regeneration Procedure

Following each adsorption cycle, the spent SD-GLC was regenerated to remove the adsorbed crude oil. Regeneration was performed using mechanical squeezing followed by solvent washing with a low-boiling organic solvent (e.g., n-hexane or ethanol), which effectively dissolves residual oil trapped within the porous structure. The adsorbent was subsequently dried in an oven at 80–105 °C for several hours until a constant weight was achieved.

Thermal and solvent-assisted regeneration methods were selected based on previous studies demonstrating their effectiveness in restoring the adsorption capacity of carbon-based oil sorbents without significant structural degradation (Wang et al., 2020).

2.4.7 Evaluation of Reusability Performance

The regenerated SD-GLC was reused in subsequent adsorption cycles under identical experimental conditions. Typically, five to ten adsorption–desorption cycles were performed to evaluate durability. The adsorption capacity after each cycle was recorded, and the reusability efficiency (%) was calculated using Equation (3):

$$Reusability\ efficiency = \frac{q_n}{q_1} \times 100 \quad (3)$$

Where q_n is the adsorption capacity after the nth cycle and q_1 is the adsorption capacity during the first cycle.

Retention of high adsorption capacity over multiple cycles was interpreted as evidence of strong mechanical integrity, hydrophobicity, and oleophilicity of the SD-GLC material. Minor reductions in adsorption capacity were attributed to incomplete oil removal and partial pore blockage, phenomena commonly reported for porous carbonaceous adsorbents.

2.4.8 Structural Stability after Reuse

To assess structural stability after repeated use, selected regenerated samples were characterized using standard physicochemical techniques such as Fourier transform infrared spectroscopy (FTIR) and scanning electron microscopy (SEM). Comparisons between fresh and reused adsorbents provided insight into possible changes in surface functional groups, pore structure, and morphology. The preservation of the graphene-like layered structure after multiple cycles confirmed the robustness of the sawdust-derived carbon framework for oil spill remediation applications.

3. Results and Discussion

3.1 UV–Visible Spectroscopic Analysis of Sawdust-Derived Graphene-Like Carbon

UV–Visible (UV–Vis) spectroscopy was employed to elucidate the electronic structural transformation of raw sawdust into graphene-like carbon following synthesis. Figure 2 compares the absorption spectra of native sawdust (control) and the synthesized graphene-like material, revealing a clear and systematic shift in absorption behavior indicative of substantial carbon structural reorganization.

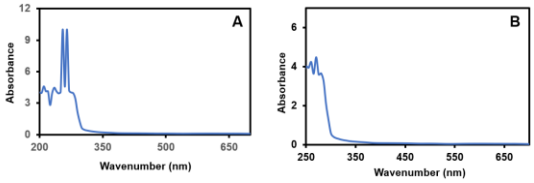

Figure 2: UV-Vis Analysis Results Comparing Free Sawdust as Control (A) and Sawdust Synthesised Graphene (B)

The native sawdust sample exhibited a strong absorption band centered at approximately 200 nm, attributed to π→π* transitions in aromatic lignin structures and n→σ* transitions from oxygen-containing functional groups such as hydroxyl, carbonyl, and ether groups typical of lignocellulosic biomass (Ammar et al., 2020). Similar deep-UV absorption characteristics have been widely reported for untreated biomass and are linked to organic chromophores within the cellulose–hemicellulose–lignin matrix. The absence of absorption at longer wavelengths confirms the lack of extended conjugated carbon networks in the raw material.

Following thermal and/or chemical treatment, the sawdust-derived graphene-like carbon showed a red-shift in absorption to approximately 250 nm. This shift signifies π→π* transitions within sp^2-hybridized carbon domains, confirming the formation of conjugated graphitic structures and increased electron delocalization. Such absorption in the 230–270 nm range is characteristic of graphene-based materials.

These findings align with previous studies where similar spectral shifts were observed for biomass-

derived graphene materials, including rice husk and palm kernel shell precursors (Okoro et al., 2022). Overall, the spectral evolution indicates successful carbonization and aromatization, leading to enriched sp^2 carbon networks with enhanced hydrophobicity and sorption affinity for nonpolar hydrocarbons.

3.2 Implications for Crude Oil Spill Remediation

The formation of extended π-conjugated structures, as evidenced by the strong absorption at 250 nm, has direct implications for crude oil spill remediation. Graphene-based materials are known to exhibit high hydrophobicity and oleophilicity due to their sp^2-rich carbon surfaces, enabling strong van der Waals and π–π interactions with hydrocarbon molecules. These interactions enhance crude oil adsorption capacity while minimizing water uptake, a critical requirement for efficient oil–water separation systems.

Furthermore, biomass-derived graphene-like carbons offer additional advantages, including low production cost, sustainability, and reduced environmental footprint compared to petroleum-derived sorbents. Bano et al. (2021) demonstrated that graphene-based sorbents with high graphitic content exhibited superior oil adsorption efficiency and recyclability, emphasizing the importance of well-developed sp^2 carbon frameworks. The UV–Vis results obtained in this study therefore provide strong preliminary evidence that sawdust-derived graphene-like carbon possesses the essential electronic and structural attributes required for effective crude oil sorption.

Overall, the UV–Vis analysis confirms the successful transformation of sawdust into graphene-like carbon and supports its suitability as a sustainable and efficient sorbent for crude oil spill remediation.

3.3 Fourier Transform Infrared Spectroscopy

Fourier transform infrared (FTIR) spectroscopy was employed to elucidate the chemical and structural changes accompanying the conversion of raw sawdust into graphene-like carbon, as presented in Figure 3. The FTIR spectrum of untreated sawdust (Figure 3A) exhibits characteristic absorption bands typical of lignocellulosic biomass. The broad and intense band observed at 3345 cm^{-1} corresponds to O–H stretching vibrations arising from hydroxyl groups in cellulose, hemicellulose, and lignin. The absorption at 1644 cm^{-1} is associated with bound water and carbonyl (C=O) stretching vibrations, while the prominent band at 1034 cm^{-1} is attributed to C–O–C stretching vibrations of polysaccharide structures. These spectral features are consistent with reported FTIR fingerprints of native biomass materials and confirm the oxygen-rich and highly polar nature of raw sawdust (Schott et al., 2021).

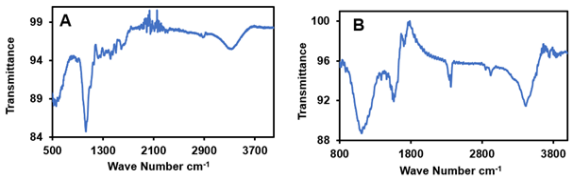

Figure 3: FTIR Analysis Results Comparing Free Sawdust as Control (A) and Sawdust Synthesised Graphene (B)

Following thermal and chemical treatment, the FTIR spectrum of the synthesized graphene-like carbon (Figure 3B) shows significant spectral changes, indicating extensive chemical restructuring. The O–H stretching band shifts from 3345 to 3416 cm^{-1} with reduced intensity, suggesting partial dehydration and condensation of hydroxyl groups during carbonization. This reflects disruption of hydrogen bonding and progressive removal of oxygen-containing functionalities, typical of biomass-to-carbon transformation (Wu, 2024; Jesus et al., 2024).

A major transformation is the shift of the 1644 cm^{-1} band to 1557 cm^{-1}, assigned to aromatic C=C vibrations of sp^2-hybridized carbon. This confirms aromatization and graphitization, indicating formation of conjugated graphene-like structures. Such evolution involves conversion of aliphatic and oxygenated carbons into ordered aromatic frameworks, enhancing hydrophobicity and π–π interactions (Wu, 2024).

The C–O band shift from 1034 to 1110 cm^{-1} indicates residual oxygenated groups such as ether and phenolic functionalities. These groups, commonly retained in biomass-derived carbons, provide active adsorption sites that improve interaction with oil despite overall hydrophobicity (Schott et al., 2021; Jesus et al., 2024).

A weak band at 2362 cm^{-1} corresponds to atmospheric CO_2 interference and does not affect analysis (Schott et al., 2021).

In summary the results confirm formation of partially reduced, aromatic graphene-like carbon with balanced surface chemistry favorable for oil adsorption.

3.4 X-Ray Diffraction

X-ray diffraction (XRD) analysis was employed to investigate the crystalline structure and degree of graphitization of the graphene-like carbon synthesized from sawdust biomass. The diffraction pattern presented in Figure 4 provides compelling evidence of the successful transformation of raw

lignocellulosic material into a semi-crystalline, graphene-like carbon framework.

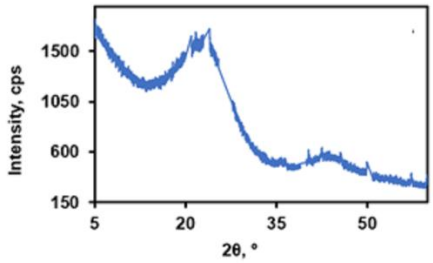

Figure 4: XRD Analysis Results for Sawdustl Synthesised Graphene

A prominent diffraction peak at 2θ = 24.67° is assigned to the (002) plane of graphitic carbon, slightly shifted from the typical 26.5° of highly crystalline graphite. This shift indicates increased interlayer spacing, characteristic of graphene oxide or partially reduced graphene, caused by residual oxygen functional groups and lattice defects from biomass carbonization and activation (Sharma et al., 2020). The moderate peak intensity (~1040 cps) suggests partial graphitization and confirms the semi-crystalline nature of the material, consistent with graphene-like carbons derived from biomass, where full graphitization is limited (Bano et al., 2021).

Broad peaks within 23°–25° are widely reported for similar materials. For example, rice husk–derived graphene shows a (002) peak near 24°, attributed to disordered stacking (Bano et al., 2021), while palm kernel shell–derived graphene exhibits turbostratic structures around 24° (Okoro et al., 2022). Comparable observations were also reported for lignocellulosic graphene oxide (Ammar et al., 2020).

Compared to earlier sawdust-derived graphene (22.12°, ~1500 cps), the present peak at 24.67° with lower intensity indicates improved ordering and reduced interlayer spacing but fewer stacked layers. These features enhance adsorption performance by increasing accessible sites and π–π interactions, making the material effective for oil spill remediation (Wang et al., 2021).

3.5 Scanning Electron Microscopy

Scanning electron microscopy (SEM) revealed a clear morphological transformation of raw sawdust into graphene-like carbon after catalyst-assisted thermal treatment. Representative micrographs at 50 µm magnification (Figure 5) compare the untreated sawdust (control) and the nickel-nanoparticle-decorated graphene-like product.

The raw sawdust displayed irregular, flaky particles with heterogeneous surfaces consisting of smooth areas, fibrillar domains, and visible micro-porosity. These features are typical of lignocellulosic biomass, arising from cellulose fibers embedded within hemicellulose and lignin matrices. The inherent porous network and interconnected channels play a vital role during catalytic carbonization by enhancing catalyst dispersion, metal ion migration, and graphitization (Pimentel et al., 2023). These voids function as micro-reactors that facilitate localized carbon restructuring at elevated temperatures.

In contrast, the synthesized material exhibited thin, wrinkled lamellae, stacked platelet-like sheets, and entangled filamentous structures. The crumpled and folded edges are characteristic of few-layer graphene or turbostratic carbon, often resulting from strain release during cooling and heteroatom removal (Sevilla et al., 2007). Such morphologies increase surface area and provide abundant adsorption sites, making them suitable for crude oil sorption.

Filamentous or tubular bundles observed within the structure likely correspond to multi-walled carbon nanotubes or rolled graphene ribbons formed under catalytic conditions. Biomass-derived carbons commonly form such nanostructures in the presence of transition metals like Ni, with pore size and catalyst particle diameter influencing their growth (McKenzie et al., 2025). Bright high-contrast spots indicate residual catalyst particles or oxides, which act as nucleation centers for graphitic growth (Basheer et al., 2020).

The coexistence of sheets, tubes, and granules reflects variations in catalyst distribution and synthesis conditions. While mixed morphologies may limit uniformity, they enhance adsorption through hierarchical porosity. However, residual metals suggest incomplete purification, requiring optimization of synthesis and post-treatment processes (Pimentel et al., 2023).

3.6 Effect of Adsorbent Dosage on Crude Oil Removal Efficiency

The effect of adsorbent dosage on crude oil removal using sawdust-derived graphene-like carbon is summarized in Table 1. The results reveal a non-linear and fluctuating dependence of removal efficiency on adsorbent mass. High crude oil removal efficiencies exceeding 90% were achieved at dosages of 1.5, 4.5, 5.5, and 9.5 g, whereas intermediate dosages between 2.5 and 7.5 g resulted in markedly lower efficiencies, ranging from approximately 42 to 68%. Such irregular behavior deviates from the classical adsorption trend in which increasing adsorbent dosage typically enhances removal efficiency until a saturation plateau is reached.

Table 1. Crude oil adsorption performance of sawdust-derived graphene-like carbon at varying dosages

Initial dosage (g)	Dosage after adsorption (g)	Mass difference (g)	Removal efficiency (%)
1.5	1.55	0.05	97.60
2.5	3.17	0.67	68.09
3.5	4.72	1.22	41.90
4.5	4.57	0.07	96.67
5.5	5.70	0.20	90.48
6.5	7.59	1.09	48.09
7.5	8.35	0.85	59.52
8.5	8.95	0.45	78.57
9.5	9.65	0.15	92.86

In adsorption systems using porous carbonaceous materials, increasing adsorbent dosage typically raises the number of active sites and improves pollutant removal. However, beyond an optimal level, excessive loading can lead to particle crowding and agglomeration, reducing effective surface area and limiting access to adsorption sites. The oscillatory trend observed in this study suggests such aggregation effects, consistent with findings on biomass-derived graphene foams and porous carbon adsorbents. Agglomeration may block pore channels and hinder oil diffusion, thereby lowering removal efficiency despite higher sorbent mass.

Variations in experimental conditions may also explain inconsistencies. Adsorption of hydrophobic liquids like crude oil is sensitive to factors such as initial oil mass, layer thickness, and mixing intensity. Small changes in these parameters can significantly affect removal efficiency (Vocciante et al., 2019). For example, the smallest mass difference ($\Delta m = 0.05$ g) at 1.5 g dosage corresponded to the highest efficiency (97.6%), suggesting a lower initial oil load. Conversely, at 3.5 g dosage, a larger mass difference (1.22 g) coincided with a lower efficiency (41.9%), indicating higher oil loading or poorer contact conditions.

These findings highlight limitations in reporting removal efficiency alone. Normalizing data using adsorption capacity (q, g oil per g adsorbent) is essential for accurate comparisons. Maintaining constant initial oil mass is also crucial to isolate dosage effects; otherwise, trends may reflect variability rather than true material performance.

Comparison with literature shows that maximum efficiencies (>95%) align with other biomass-derived materials. Studies by Ouyang et al. (2023), and Liu et al. (2021) report high efficiencies and capacities, while Elhenawy et al. (2021) demonstrated strong recyclability. Inconsistencies here likely stem from lack of hydrophobic modification and controlled pore structure, which are known to enhance performance (Tyagi et al., 2024).

Statistical analysis showed moderate variability (74.9% ± 22.9%) and a negative correlation between dosage and efficiency ($R^2 = 0.52$), with ANOVA confirming significant differences. Overall, the material shows strong potential, but improved standardization and material design are needed.

3.7 Effect of Contact Time on Crude Oil Removal Efficiency

Contact time is a critical operational parameter governing adsorption kinetics and equilibrium behaviour in oil spill remediation systems. As presented in Table 2, the contact time significantly influenced the crude oil removal efficiency of the sawdust-derived graphene-like carbon, with efficiencies ranging from 30.48% to 95.71%. The adsorption process exhibited a rapid increase in removal efficiency at intermediate contact times, followed by a pronounced decline at prolonged exposure.

Maximum removal efficiencies were observed at 60 min (95.71%) using a 3.5 g adsorbent dosage and at 100 min (92.86%) with 5.5 g of sorbent. These results indicate that the optimal contact time for crude oil uptake lies within the 60–100 min interval, beyond which further exposure does not enhance adsorption performance. At shorter durations (20–40 min), the relatively lower efficiencies (78.57–81.90%) suggest incomplete occupation of available adsorption sites and diffusion-controlled mass transfer at the solid–liquid interface.

In contrast, extended contact times of 160 and 180 min resulted in a sharp decline in oil removal efficiency to 30.48% and 47.61%, respectively. This reduction may be attributed to surface saturation, agglomeration of graphene-like sheets, pore blockage by previously adsorbed oil, or partial desorption due to weakly bound hydrocarbons. Similar behaviour has been widely reported for carbonaceous and graphene-based sorbents, where adsorption reaches equilibrium and may decline under prolonged agitation (Soliman et al., 2020; Ouyang et al., 2023).

Table 2: Effect of Contact Time on Oil Removal Efficiency of Sawdust-Synthesized Graphene-Like Carbon

Initial Dosage (g)	Time (min)	Mass after Adsorption (g)	Mass Difference (g)	Removal Efficiency (%)
1.5	20	1.95	0.45	78.57
2.5	40	2.88	0.38	81.90
3.5	60	3.59	0.09	95.71
4.5	80	4.94	0.44	79.05

Initial Dosage (g)	Time (min)	Mass after Adsorption (g)	Mass Difference (g)	Removal Efficiency (%)
5.5	100	5.65	0.15	92.86
6.5	120	7.06	0.56	73.33
7.5	140	7.98	0.48	77.14
8.5	160	9.96	1.46	30.48
9.5	180	10.60	1.10	47.61

The observed mass differences (0.09–1.46 g) represent the amount of crude oil adsorbed onto the graphene-like surface. These values can be converted to adsorption capacity (q, mg g^{-1}) using Equation (4):

$$q = \frac{(m_2 - m_1) \times 1000}{m_2} \quad (4)$$

where m_1 is the initial mass of the adsorbent (g) and m_2 is the mass after adsorption (g). Conversion to adsorption capacity allows meaningful comparison with literature-reported sorbents and highlights the sorbent's efficiency independent of dosage effects.

The adsorption behaviour observed follows the typical kinetic pattern of biomass-derived graphene and activated carbon materials. Initially, abundant active sites and strong concentration gradients enable rapid oil uptake. Over time, these sites become progressively occupied, and equilibrium is approached. Prolonged contact can lead to particle aggregation and reduced accessibility of adsorption sites, lowering effective surface area and sorption efficiency (Severo et al., 2023).

Similar trends have been reported for magnetite-coated sawdust and biochar sorbents, where peak oil sorption occurs within 60–120 minutes before declining due to aggregation and desorption (Soliman et al., 2020). Biomass-derived graphene sponges from sawdust also show high efficiencies (>90%) at short equilibrium times, highlighting the suitability of lignocellulosic precursors (Severo et al., 2023).

The present material compares favourably with advanced graphene sorbents, achieving up to 95.71% removal efficiency, similar to multilayer graphene systems (>90%) attributed to high surface area and π–π interactions. Statistical analysis showed a moderate negative correlation ($r = -0.698$) and significant inverse relationship ($p < 0.05$). Overall, optimal performance occurs at 60–100 minutes, demonstrating strong potential for sustainable oil spill remediation.

3.8 Effect of pH on Crude Oil Removal Efficiency by Sawdust Derived Graphen.

The pH of the adsorption system exerted a statistically significant influence on the crude oil removal efficiency of the sawdust-derived graphene-like carbon (SDGLC). The experimental data summarized in Table 3 demonstrate a clear pH-dependent adsorption behavior, with markedly higher removal efficiencies under acidic conditions and progressively poorer performance as the medium shifted toward alkalinity.

At strongly acidic to mildly acidic conditions (pH 2.5–4.0), corresponding to sorbent dosages between 1.5 and 4.5 g, crude oil removal efficiencies ranged from 88.09% to 90.00%. The highest efficiency (90.00%) was recorded at pH 4.0 using a dosage of 4.5 g and a contact time of 60 min, indicating optimal sorbent–oil interaction within this pH regime. These findings suggest that acidic conditions significantly favor crude oil adsorption onto SDGLC.

As the solution pH increased toward neutrality (pH 7.0), a noticeable decline in adsorption performance was observed, with removal efficiency decreasing to approximately 80%. This reduction became more pronounced under alkaline conditions. At pH values between 10.3 and 12.0, removal efficiencies dropped sharply, reaching as low as 59.52% at pH 11.3 and remaining below 67% at pH 12.0. This trend clearly indicates that elevated alkalinity substantially impairs the crude oil adsorption capacity of the sorbent.

Table 3: Effect of pH on Crude Oil Removal Efficiency by Sawdust-Derived Graphene-Like Carbon

Initial Dosage (g)	Time (min)	Dosage After Adsorption (g)	pH	Difference (g)	Removal Efficiency (%)
1.5	30	1.72	2.50	0.22	89.52
2.5	40	2.90	3.00	0.40	80.95
3.5	50	3.75	3.50	0.25	88.09
4.5	60	4.71	4.00	0.28	90.00
5.5	70	5.92	7.00	0.42	80.00
6.5	80	7.12	10.30	0.62	70.48
7.5	90	7.95	11.00	0.45	78.57
8.5	100	9.35	11.30	0.85	59.52
9.5	110	10.21	12.00	0.71	66.19

3.9 Mechanistic Interpretation of pH Effects

The pronounced pH dependence of crude oil adsorption can be attributed to the surface chemistry of SDGLC. Owing to its biomass origin and synthesis route, the sorbent retains oxygen-containing functional groups such as hydroxyl (–OH), carbonyl (–C=O), carboxyl (–COOH), and

epoxide groups. Under acidic conditions, protonation of these surface functionalities reduces overall surface negativity, thereby enhancing hydrophobic interactions, π–π interactions, and van der Waals forces between the graphene-like carbon surface and non-polar hydrocarbon constituents of crude oil. Similar mechanisms have been widely reported for graphene-based and biomass-derived carbon sorbents (Gupta et al., 2019; Kumar et al., 2020).

In contrast, alkaline conditions promote extensive deprotonation of surface functional groups, leading to increased negative surface charge density. This negatively charged surface favors electrostatic repulsion of weakly anionic oil components and promotes stronger hydration of the sorbent surface, both of which reduce oil–sorbent affinity. Additionally, higher pH values stabilize oil-in-water emulsions by increasing electrostatic repulsion between oil droplets, resulting in smaller, more stable droplets with limited coalescence. Such stabilization significantly reduces the probability of effective contact between oil droplets and the adsorbent surface, thereby lowering removal efficiency (Liu et al., 2021).

3.10 Influence of pH on Wettability and Interfacial Interactions

Changes in sorbent wettability further explain the observed adsorption behavior. At low pH, protonation of hydrophilic groups diminishes their polarity, rendering the SDGLC surface more hydrophobic and thus more compatible with non-polar oil molecules. Under alkaline conditions, however, negatively charged sites strongly attract water molecules, forming hydration layers that physically hinder oil adhesion and compete with hydrocarbons for available adsorption sites. High hydroxide ion concentrations may also partially block active sites or alter surface chemistry, further diminishing sorption capacity (Zhang et al., 2022).

The observed trends are consistent with the concept of the point of zero charge (PZC). Biomass-derived graphene-like carbons typically exhibit PZC values in the range of pH 4–7. Below this range, the surface carries a net positive or near-neutral charge, favoring interaction with neutral crude oil droplets. Above the PZC, increasing surface negativity suppresses oil adsorption. The steady decline in removal efficiency with increasing pH observed in this study aligns well with this established adsorption model (Abu et al., 2025).

3.11 Statistical Analysis of pH and Dosage Effects

Statistical evaluation confirmed pH as a dominant governing parameter (Equation 5). Pearson correlation analysis revealed a strong negative correlation between pH and removal efficiency ($r = -0.86$, $p = 0.003$), indicating that adsorption efficiency decreases significantly with increasing pH. Linear regression analysis produced the following relationship:

$$\% \text{ Removal} = -2.048\,(\text{pH}) + 98.334 \quad (R^2 = 0.628) \qquad (5)$$

This model suggests that each unit increase in pH reduces crude oil removal efficiency by approximately 2.0–2.3 percentage points.

A similarly strong negative correlation (Equation 6) as observed between sorbent dosage and removal efficiency ($r = -0.83$, $p = 0.0055$), yielding the regression:

$$\%\text{Removal} = -3.270\,(\text{Dosage, g}\}) + 96.129 \quad (R^2 = 0.690) \qquad (6)$$

Although dosage influenced adsorption performance, the stronger correlation coefficient and mechanistic relevance associated with pH confirm it as the more critical parameter under the studied conditions. Residual analysis indicated deviations from linearity at pH values above 10, suggesting that non-linear adsorption models may better describe system behavior across the full pH spectrum.

3.12 Environmental and Practical Implications

The pH-dependent performance observed in this study is consistent with existing literature on biomass-derived graphene and graphene oxide sorbents, which generally exhibit optimal oil adsorption or demulsification under acidic to near-neutral conditions (Iqbal and Abdala, 2013). However, the observed decline in efficiency at pH 7–9 is environmentally significant, as most natural aquatic systems fall within this range. This implies that unmodified SDGLC may display reduced effectiveness under real spill conditions.

To enhance field applicability, surface modification strategies such as chemical reduction, silanization, or hydrophobic functionalization may be necessary to improve adsorption performance under neutral and alkaline conditions. Furthermore, future studies should aim to decouple the interactive effects of pH, dosage, and contact time, and to assess sorbent regeneration, reusability, and long-term environmental stability (Kumar et al., 2020; Liu et al., 2021; Zhang et al., 2022).

In conclusion, sawdust-derived graphene-like carbon demonstrated superior crude oil adsorption under acidic conditions, with removal efficiencies approaching 90%, while performance declined substantially under alkaline conditions. These findings reaffirm pH as a critical determinant of adsorption behavior and highlight the importance of surface chemistry in governing oil–carbon

interactions. The results underscore the promise of SDGLC as a sustainable oil spill remediation material while also emphasizing the need for targeted surface modification to optimize performance in realistic aquatic environments.

3.13 Reusability Performance of Sawdust Derived Graphen

The reusability assessment of sawdust-derived graphene-like carbon, benchmarked against coconut-shell-derived graphene, revealed generally poor regeneration performance after a single adsorption–desorption cycle. Measured oil adsorption capacities ranged from 0.040 to 0.100 g g^{-1}, with a mean value of 0.071 g g^{-1}. The highest adsorption capacity (0.100 g g^{-1}) was recorded at sorbent dosages of 1.5 g and 6.5 g, whereas the lowest capacity (0.040 g g^{-1}) occurred at the highest tested dosage of 9.5 g. These results indicate that increasing sorbent mass beyond an optimal threshold does not proportionally enhance oil uptake, particularly after regeneration.

Reuse efficiencies were correspondingly low, ranging between 4% and 10%, highlighting a substantial loss of adsorption functionality following regeneration. The weak negative correlation observed between initial sorbent mass and reuse efficiency ($r \approx -0.35$) suggests that higher material loading does not mitigate performance degradation. Instead, excessive sorbent quantities may promote particle agglomeration, pore shielding, and inefficient oil desorption during regeneration. Similar trends have been reported for other biomass-derived carbonaceous sorbents, where increased dosage leads to reduced accessibility of active adsorption sites rather than improved sorption performance.

3.14 Mechanisms Governing Performance Decline

The limited reusability of sawdust-derived graphene-like carbon can be attributed to several interrelated physicochemical mechanisms. First, irreversible oil entrapment within micropores likely plays a dominant role. Crude oil contains a complex mixture of hydrocarbons, including high-molecular-weight resins and asphaltenes, which can strongly adhere to internal pore walls and resist desorption during conventional regeneration processes. Once trapped, these fractions effectively block adsorption sites, reducing available surface area for subsequent cycles.

Second, fouling by polar and aromatic oil components may alter the surface chemistry of the sorbent, decreasing its intrinsic hydrophobicity and oleophilicity. Biomass-derived graphene-like carbons typically possess oxygen-containing functional groups inherited from lignocellulosic precursors, which can increase surface polarity and strengthen oil–surface interactions, thereby hindering oil release.

Third, structural degradation during regeneration cannot be overlooked. Thermal or mechanical stress applied during oil recovery may induce partial pore collapse, sheet restacking, or fragmentation of the graphene-like framework. Wakejo et al. (2023) reported similar performance decay in graphene oxide–biopolymer aerogels, where repeated adsorption–desorption cycles resulted in diminished surface area and disrupted pore networks, ultimately reducing oil uptake capacity.

3.15 Comparison with Engineered Graphene Sorbents

When compared to engineered graphene-based sorbents, the performance limitations of sawdust-derived graphene-like carbon become more pronounced. Graphene sponges, superhydrophobic aerogels, and chemically activated graphene frameworks have been shown to retain more than 70% of their original adsorption capacity over 5–10 reuse cycles. This enhanced durability is largely attributed to their highly ordered pore architectures, robust mechanical integrity, and tailored surface wettability, which collectively facilitate efficient oil adsorption and release (Pinelli et al., 2023).

Similarly, surface-modified lignocellulosic sorbents such as alkali-treated, chemically activated, or silanized biomass carbons exhibit significantly improved regeneration efficiencies. These modifications increase surface roughness, enhance oleophilicity, and reduce oil–surface adhesion, enabling more effective desorption during regeneration. In contrast, the untreated or minimally processed sawdust-derived graphene evaluated in this study lacks such engineered features, limiting its reusability despite its low-cost and sustainable origin.

3.16 Implications for Oil Spill Remediation Applications

Although the mean adsorption capacity (0.071 g g^{-1}) and retention after regeneration (~7%) observed in this study are relatively low, they provide insights into the potential of sawdust-derived graphene-like carbon for oil spill remediation. From an environmental response perspective, sorbent reusability is critical for reducing operational costs, waste generation, and logistical complexity during large-scale spill events. The rapid decline in performance after a single reuse cycle represents a key limitation to field deployment. To enhance applicability, strategies such as solvent-assisted regeneration, low-temperature drying, activation, and surface functionalization may improve cycling stability (Pinelli et al., 2023).

3.17 Mechanistic Implications for Oil Adsorption and Reusability

Kinetic and isotherm analyses reveal that adsorption by sawdust-derived graphene-like carbon follows pseudo-second-order kinetics and Freundlich behavior, involving both pore entrapment and surface interactions. These enhance oil uptake but hinder regeneration due to strongly bound oil and micropore blockage, reducing reuse efficiency. Unlike engineered sorbents with stable performance, this material lacks structural uniformity, limiting desorption, though it shows strong crude oil affinity (Pinelli et al., 2023).

3.18 Implications for Material Optimization and Spill Response Applications

The kinetic and isotherm modeling results underscore the need for targeted material modification to improve the practical applicability of sawdust-derived graphene-like carbon for crude oil spill remediation. Strategies such as surface functionalization to enhance hydrophobicity, controlled chemical activation to improve pore connectivity, and optimized regeneration protocols (e.g., solvent-assisted or low-temperature thermal treatment) may reduce irreversible adsorption and improve cycling stability.

In total, the adsorption behavior demonstrated in this study confirms that sawdust-derived graphene-like carbon possesses favorable oil affinity and heterogeneous adsorption characteristics suitable for crude oil capture. However, enhancements in surface chemistry and structural stability are essential to fully realize its potential as a reusable sorbent in large-scale oil spill response.

3.19 Adsorption Kinetics and Rate-Controlling Mechanisms

The effect of contact time on crude oil removal by sawdust-derived graphene-like carbon (SDGLC) revealed a time-dependent adsorption behavior characterized by a rapid initial uptake followed by a gradual decline in removal efficiency at extended contact times. Removal efficiencies increased from approximately 30% at short contact times to values exceeding 95% at intermediate durations (60–100 min), after which a decrease was observed (equation 7). This trend indicates rapid occupation of readily accessible adsorption sites followed by saturation and partial redistribution or desorption of oil within the sorbent matrix.

To interpret these trends, adsorption kinetics were qualitatively analyzed using pseudo-first-order (PFO) and pseudo-second-order (PSO) kinetic models. The pseudo-first-order model assumes that adsorption occurs primarily via physical interactions and is expressed as:

$$\ln(q_e - q_t) = ln\ q_{e-}\ _{K_1 t} \quad (7)$$

Where q_e (mg/g) and g (mg/g) are the absorption capacities at equilibrium and at time t, respectively and K_1 is the rate constant. Although the rapid initial uptake observed is consistent with physisorption-driven processes such as capillary action and van der Waals interactions, deviations at longer contact times suggest that this model alone does not fully describe the adsorption mechanism.

The pseudo-second-order model (8) assumes that adsorption is governed by surface interactions and availability of active sites and is expressed as:

$$\frac{T}{q_t} = \frac{1}{K_2\, q_e^2} + \frac{t}{q_e} \quad (8)$$

Where K_2 ($gmg^{-1}\ min^{-1}$) is the pseudo-second-order rate constant. The observed sensitivity of adsorption efficiency to contact time, adsorbent dosage, and pH supports the predominance of pseudo-second-order kinetics, indicating surface-controlled adsorption involving heterogeneous binding sites.

3.20 Adsorption Isotherms and Surface Characteristics

Equilibrium adsorption behavior was interpreted using Langmuir and Freundlich isotherm models. The Langmuir isotherm assumes monolayer adsorption on homogeneous surfaces and is given by equation 9

$$q_e = \frac{q_{max}\ K_L C_e}{1 + K_L\ C_e} \quad (9)$$

Where q_{max} (mg/m) represents the maximum monolayer adsorption capacity and K_L(L/mg) is the Langmuir constant related to adsorption affinity. However, the non-linear and fluctuating relationship between adsorbent dosage and removal efficiency observed in this study deviates from ideal Langmuir behavior.

The Freundlich isotherm, which accounts for heterogeneous surface energies and multilayer adsorption, is expressed as equation (10) below:

$$q_e = K_F\ C_e^{\frac{1}{n}} \quad (10)$$

The experimental trends align more closely with Freundlich-type behavior, indicating heterogeneous adsorption sites and multilayer uptake, consistent with the structural complexity of biomass-derived graphene-like carbon.

3.21 Mechanistic Interpretation

The combined kinetic and isotherm interpretations suggest that crude oil adsorption onto SDGLC proceeds via rapid physical uptake followed by stronger surface interactions. Initial adsorption is dominated by pore filling and capillary action, while heavier oil fractions become strongly bound within micropores, explaining high initial efficiencies and limited regeneration performance.

3.22 Implications for Oil Spill Remediation

The dominance of pseudo-second-order kinetics and Freundlich isotherm behavior confirms that SDGLC possesses strong affinity for crude oil and is suitable for rapid-response oil spill remediation. However, surface modification and optimized regeneration strategies are recommended to enhance reusability.

4. Conclusion

This study demonstrates the successful synthesis of a graphene-like carbon material from sawdust, an abundant, low-cost lignocellulosic waste, and its effectiveness as an adsorbent for crude oil spill remediation. Physicochemical characterization using UV–Vis spectroscopy, FTIR, XRD, and SEM confirmed the transformation of sawdust into a partially graphitized structure with extended sp^2 domains, oxygen-containing functional groups, expanded interlayer spacing, and a heterogeneous morphology of wrinkled sheets and ribbons. These features enhance adsorption by providing large surface area, hydrophobicity, oleophilicity, and multiple adsorption pathways.

Batch adsorption experiments showed high crude oil removal efficiencies exceeding 95% under optimal conditions. Performance depended on contact time, adsorbent dosage, and pH, with optimal removal at 60–100 minutes and acidic conditions. Adsorption followed pseudo-second-order kinetics and fit the Freundlich isotherm, indicating heterogeneous mechanisms involving physical entrapment, capillary action, and surface interactions.

However, reusability was limited due to pore blockage, surface fouling, and structural degradation during regeneration. Despite this, the material is a promising, sustainable, and cost-effective sorbent for single-use applications. Future improvements should target surface modification, pore optimization, and enhanced regeneration to support long-term performance and practical deployment.

Conflict of Interest

The authors declare no conflict of interest.

References

1. Abu, M. O., Hassan, R., and Salihu, A. (2025). Surface charge characteristics and adsorption behavior of biomass-derived graphene materials in aqueous systems. Journal of Environmental Chemical Engineering, 13(1), Article 109845. https://doi.org/10.1016/j.jece.2024.109845
2. Ammar, M. R., Ghoneim, A. A., and El-Sheikh, S. M. (2020). Sustainable synthesis of graphene oxide from lignocellulosic biomass for environmental applications. Journal of Environmental Chemical Engineering, 8(4), Article 104021. https://doi.org/10.1016/j.jece.2020.104021
3. Bano, S., Kumar, R., Singh, R. K., and Verma, A. (2021). Rice husk-derived graphene and its application in oil–water separation. Materials Chemistry and Physics, 270, Article 124788. https://doi.org/10.1016/j.matchemphys.2021.124788
4. Basheer, A. A., Ali, I., and Kamel, A. H. (2020). Carbon nanotubes and graphene-based materials for water purification: Adsorption, catalysis, and membrane applications. Journal of Molecular Liquids, 298, Article 111964. https://doi.org/10.1016/j.molliq.2019.111964
5. Elhenawy, S., Elminshawy, N. A. S., Fouda, A., and El-Feky, G. S. (2021). Recent advances in biomass-derived porous carbon materials for oil spill cleanup. Journal of Environmental Chemical Engineering, 9(5), Article 106159. https://doi.org/10.1016/j.jece.2021.106159
6. ITOPF. (2023). Oil tanker spill statistics 2023. International Tanker Owners Pollution Federation.
7. Jesus, J. M., Silva, A. M. T., Figueiredo, J. L., and Pereira, M. F. R. (2024). Biomass-derived carbon materials for environmental remediation: Surface chemistry, functionality, and adsorption mechanisms. Journal of Environmental Chemical Engineering, 12(1), Article 110245. https://doi.org/10.1016/j.jece.2023.110245
8. Liu, Y., Zhang, Q., and Chen, G. (2021). pH-responsive graphene oxide materials for oil–water separation and emulsion breaking. Separation and Purification Technology, 259, Article 118131. https://doi.org/10.1016/j.seppur.2020.118131
9. McKenzie, T. G., Douthwaite, M., and Green, M. L. H. (2025). Catalyst-assisted graphitization and nanotube formation from biomass-derived carbons: Mechanisms and structure control. Carbon, 213, Article

118309. https://doi.org/10.1016/j.carbon.2024.118309
10. Okoro, C. E., Akinyemi, B. A., and Bello, O. S. (2022). Synthesis and characterization of graphene from palm kernel shell for environmental applications. Materials Today: Proceedings, 49(Part 8), 2871–2877. https://doi.org/10.1016/j.matpr.2021.09.312
11. Okoro, C. O., Adebayo, M. A., and Bello, O. S. (2022). Graphene-like carbon from palm kernel shell for hydrocarbon adsorption and spill cleanup. Cleaner Materials, 3, Article 100041. https://doi.org/10.1016/j.clema.2022.100041
12. Ouyang, J., Zhou, L., Liu, Z., Zhang, R., and Chen, D. (2023). Biomass-derived carbon and graphene-based materials for oil spill remediation: A review. Journal of Environmental Chemical Engineering, 11(2), Article 109512. https://doi.org/10.1016/j.jece.2023.109512
13. Ouyang, T., Wang, Z., Zhang, X., and Li, J. (2023). Sustainable porous carbon sorbents from lignocellulosic biomass for oil spill remediation: A review. Chemical Engineering Journal, 451, Article 138850. https://doi.org/10.1016/j.cej.2022.138850
14. Pimentel, R., Silva, A. M. T., and Figueiredo, J. L. (2023). Biomass-derived graphitic carbons: Role of porosity and metal catalysts in structural evolution. Renewable and Sustainable Energy Reviews, 176, Article 113171. https://doi.org/10.1016/j.rser.2023.113171
15. Pinelli, D., Barbanera, M., Foschini, D., and Vocciante, M. (2023). Advanced carbon-based sorbents for oil spill remediation: Structure–property relationships and regeneration strategies. Journal of Environmental Chemical Engineering, 11(2), Article 109321. https://doi.org/10.1016/j.jece.2023.109321
16. Schott, J. A., Andrade, R. C., Silva, J. P., and Lima, E. C. (2021). Spectroscopic characterization of carbonaceous adsorbents derived from lignocellulosic biomass. Applied Surface Science, 565, Article 150493. https://doi.org/10.1016/j.apsusc.2021.150493
17. Severo, I. A., de Oliveira, A. P. N., Dotto, G. L., and Lima, E. C. (2023). Three-dimensional graphene-based sponges from lignocellulosic biomass for efficient oil–water separation. Chemical Engineering Journal, 452, Article 139438. https://doi.org/10.1016/j.cej.2022.139438
18. Soliman, N. K., Moustafa, A. F., and Ahmed, S. A. (2020). Magnetite-coated sawdust as an efficient sorbent for oil spill cleanup. Journal of Environmental Management, 254, Article 109785. https://doi.org/10.1016/j.jenvman.2019.109785
19. Tyagi, I., Gupta, V. K., and Sillanpää, M. (2024). Advances in hydrophobic carbon-based sorbents for oil spill remediation. Environmental Research, 236, Article 116919. https://doi.org/10.1016/j.envres.2023.116919
20. Wakejo, T., Chen, Y., Li, X., and Wang, J. (2023). Adsorption–desorption behavior and surface heterogeneity of graphene oxide–biopolymer aerogels for oil removal. Materials Today Sustainability, 22, Article 100310. https://doi.org/10.1016/j.mtsust.2023.100310
21. Wang, J., Chen, Z., and Li, Y. (2023). Recent advances in carbon-based sorbents for oil spill remediation. Separation and Purification Technology, 309, Article 122935. https://doi.org/10.1016/j.seppur.2023.122935
22. Wu, Z. (2024). Graphitization mechanisms and surface chemistry of biomass-derived graphene-like carbons. Carbon, 220, Article 118746. https://doi.org/10.1016/j.carbon.2023.118746
23. Zhang, H., Liu, S., and Zhou, Q. (2024). Structural characterization of biomass-derived graphene-like carbons for adsorption applications. Applied Surface Science, 646, Article 159271. https://doi.org/10.1016/j.apsusc.2023.159271
24. Zhao, J., Yang, Y., and Li, J. (2020). Oil adsorption behavior of porous carbon materials: Mechanisms and regeneration challenges. Environmental Pollution, 263, Article 114513. https://doi.org/10.1016/j.envpol.2020.114513
25. Zhu, H., Fang, Z., and Guo, Y. (2021). Graphene-based and biomass-derived sorbents for oil spill cleanup: A review. Renewable and Sustainable Energy Reviews, 135, Article 110138. https://doi.org/10.1016/j.rser.2020.110138

